The effect of temperature and strain rate on the deformation behaviour, structure development and properties of biaxially stretched PET-clay nanocomposites

Yucai Shen, Eileen Harkin-Jones, Peter Hornsby, Tony Mcnally, Rund Abu-Zurayk

The effect of temperature and strain rate on the deformation behaviour, structure development and properties of biaxially stretched PET-clay nanocomposites

Yucai Shen, Eileen Harkin-Jones, Peter Hornsby, Tony McNally, Rund Abu-Zurayk

PII: S0266-3538(11)00052-2
DOI: 10.1016/j.compscitech.2011.01.024
Reference: CSTE 4919

To appear in: *Composites Science and Technology*

Received Date: 21 December 2010
Revised Date: 27 January 2011
Accepted Date: 30 January 2011

Please cite this article as: Shen, Y., Harkin-Jones, E., Hornsby, P., McNally, T., Abu-Zurayk, R., The effect of temperature and strain rate on the deformation behaviour, structure development and properties of biaxially stretched PET-clay nanocomposites, *Composites Science and Technology* (2011), doi: 10.1016/j.compscitech.2011.01.024

The effect of temperature and strain rate on the deformation behaviour, structure development and properties of biaxially stretched PET-clay nanocomposites

Yucai Shen, Eileen Harkin-Jones*, Peter Hornsby, Tony McNally, Rund Abu-Zurayk

School of Mechanical & Aerospace Engineering, Queen's University Belfast, BT9 5AH, UK

Abstract

The inclusion of a synthetic fluoromica clay in PET affects its processability via biaxial stretching and stretching temperature (95 °C and 102 °C) and strain rate (1 s^{-1} and 2 s^{-1}) influence the structuring and properties of the stretched material. The inclusion of clay has little effect on the temperature operating window for the PET-clay but it has a major effect on deformation behavior which will necessitate the use of much higher forming forces during processing. The strain hardening behavior of both the filled and unfilled materials is well correlated with tensile strength and tensile modulus. Increasing the stretching temperature to reduce stretching forces has a detrimental effect on clay exfoliation, mechanical and O_2 barrier properties. Increasing strain rate has a lesser effect on the strain hardening behavior of the PET-clay compared with the pure PET and this is attributed to possible adiabatic heating in the PET-clay sample at the higher strain rate. The Halpin-Tsai model is shown to accurately predict the modulus enhancement of the PET-clay materials when a modified particle modulus rather than nominal clay modulus is used.

Keywords: A. Nanoclays, A. Nanocomposites, D. Transmission electron microscopy (TEM) B. Mechanical properties

*Corresponding author. Tel.: +44 (0)28 9097 4490
E-mail address: e.harkinjones@qub.ac.uk

1 Introduction

Polymer-clay nanocomposites address some of the shortcomings of polymers for conventional composites for both packaging and engineering applications requiring enhanced mechanical, barrier and high temperature performance [1]. Since these superior properties may be realized with relatively low clay loadings, the materials are also much lighter compared to conventional polymer composites. This advantage could have a significant impact on alleviating concerns about the environmental impact of plastic packaging by reducing pack weight as well as the energy required to process and transport it. Despite the huge research interest in polymer-clay nanocomposites, studies on the processing of these materials have been largely confined to the effects of extrusion conditions (shear flow) on the melt processed polymer-clay structure and properties [2-5].

A key observation in some of this work has been that shear flow may have a negligible effect on the exfoliation of clay if the polymer-clay affinity is low [3]. This is important in packaging where polyolefins and other non polar polymers play a major role. On the other hand, studies on polyethylene fibres reinforced with clay have shown that elongational flow in the melt state can induce exfoliation in polymer-clay nanocomposites even if there is a low polymer-clay affinity [6]. Since the majority of packaging is actually formed via secondary processes involving extensional deformation it is important that we gain an understanding of how polymer-clay composites behave under this type of deformation and how structure and properties are influenced. Biaxial deformation of sheet material in the semi-solid state is typical of the thermoforming and injection stretch blow moulding processes and relatively few studies have been carried out in this area [7-9]. Earlier studies at Queen's University Belfast [7, 8] have shown that biaxial stretching increases the degree

of exfoliation for both PP-clay and PET-clay nanocomposites resulting in enhanced mechanical and barrier properties. The addition of clay to PET also had a large effect on the strain hardening behaviour of PET but not on PP [7, 8]. In this present study we extend the investigation of PET-clay nanocomposites processability and structuring with a more detailed study of the influence of stretching temperature and strain rate on clay dispersion, polymer morphology and mechanical and barrier properties.

2 Experimental

2.1 Materials

The PET used was ARTENIUS PURA PET with an intrinsic viscosity of 0.74 dl/g. A synthetic fluoromica clay modified with 31% methyl trioctyl ammonium chloride, Somasif MTE from Uni-Coop Japan, with a nominal diameter in the region of 1000 nm was used.

2.2 Preparation

The stretch blow moulding and thermoforming of PET typically involves the production of an amorphous "preform" which is subsequently heated above its glass transition temperature (T_g) and then formed into a mould via a biaxial stretching process to form the final part. In this study we replicate the industrial process by producing a quenched PET sheet by compression moulding, heating the sheet above its T_g and then biaxially stretching it. Ground PET powder was dried in a dehumidifying dryer at 120 °C for 24 hours and it was mixed with the clay, at a loading of 6 wt%. All materials were then compounded in a Haake co-rotating twin screw extruder (Rheomex OS PTW16) with a screw diameter of 16 mm and L/D of 25 with a temperature profile of 265, 275, 275, 270, 270, 265 °C from zones 1 to 6. The extruded filament was cooled in a water bath and pelletized. The screw speed was set at 120 rpm and the feeding rate was 7 %. The extruded pellets were

compression moulded, in a steel mould of 1 mm thickness at 260 °C for 2.5 minutes in a Dr Collin P200P platen press machine. The material was quenched by inserting two water-cooled cassettes between the platens. Biaxial stretching of the compression moulded sheet was conducted in a biaxial tester developed in-house at Queen's University Belfast [10]. Samples with dimension of 76 mm × 76 mm and 1 mm thickness were clamped by pneumatic grips and then heated by hot air blowers positioned above and below the sheet to achieve a uniform temperature. Heating was stopped after the required time and the sample was then stretched equi-biaxially. The sample was cooled to room temperature in ambient air at the end of each test. The stretching parameters used are shown in Table 1.

2.3 Characterization

TEM

Samples for TEM were cut into 50 nm slices using a Reichert Jung Ultracut-E microtome with a diamond knife. TEM images were obtained using a Philips CM 100 TEM instrument recorded at 200 kV accelerating voltage at different magnifications.

DSC

Differential scanning calorimetric (DSC) thermograms were recorded using a Perkin Elmer DSC 6 under a nitrogen atmosphere. The sample of 5 - 6 mg was placed in an aluminium pan and sealed using a press. The samples were heated from 30 - 285 °C at a heating rate of 283 K/min. For low crystalline PET, cold crystallization can occur during the first heating of the DSC testing, resulting in an exothermic peak. The percent crystallinity was therefore calculated as in Fan et al [11]. For PET, ΔH_m^o was taken as 140 J/g [12].

XRD

A Philips X'Pert type PW3040 X-ray diffractometer was used to determine the d-spacing between the clay platelets. Cu-Kα radiation with a wavelength of 1.54 Å was used. Data were collected from 1 to 40º. The d-spacing (the distance between the basal layers of the clay) was determined using Bragg's law.

Tensile testing

Tensile tests were carried out (BS EN ISO 527: 1996) using an Instron 5564 Universal Tester at room temperature. Tensile modulus values were determined using a clip-on extensometer at a crosshead speed of 1 mm/min. Strength and elongation values were taken at a crosshead speed of 50 mm/min. At least five samples were tested at each condition.

Oxygen barrier testing

A Mocon Oxtran model 2/21 oxygen barrier tester was used to measure oxygen gas transmission rate. The test area for the sample was 1 cm^2 using an aluminium mask. The test conditions were 23 °C, 0 % relative humidity and atmospheric pressure. A test was started after conditioning for 5 h and the oxygen transmission rate was recorded in the steady state when the sample had equilibrated.

3 Results and discussion

3.1 DSC and XRD results for compression moulded sheet (the "preform")

It can be observed in Table 2 that the d-spacing of the PET-clay sample is somewhat less than that of the original clay. This may indicate that some degradation of the surfactant has taken place during melt processing. The crystallinity and melting temperature of the samples are not much affected by the addition of clay and there is only a slight decrease in cold crystallisation temperature and glass transition temperature. Overall, the temperature

operating window (i.e. T_{cc} - T_g) for polymer processing is not significantly affected by the addition of clay.

3.2 Biaxial deformation behaviour

Figure 1 shows the biaxial deformation behaviour of the materials stretched at a strain rate of 1 s^{-1} to a stretch ratio of 3, and at different temperatures. Generally, at both temperatures, the stretching stress increases with the addition of clay, with the nanocomposites exhibiting an enhanced strain hardening behaviour compared with the pure PET. At a stretch ratio of 3 the stretching stress is increased by 53 % at 95 °C and by 46 % at 102 °C. It is well known that a typical deformation curve for PET, stretched above its glass transition temperature, shows an upswing at a particular stretch ratio. This upswing indicates the onset of strain-hardening, and the region above the upswing in stress is known as the strain-hardening region. A strain hardening parameter, SHP, can be determined from the intersection point of the line tangent to the plateau region and upswing region in the deformation curve, which is expressed in terms of stretch ratio, as proposed by Chandran and Jabarin [13]. An example showing the determination of the SHP in pure PET stretched at 102 °C, is shown in Figure 1, and all the SHP values for the stretched samples are compared in Table 3.

It is apparent that the addition of clay to the PET has the effect of decreasing the onset of strain hardening to lower strains (i.e lower values of SHP). At 95 °C the SHP is reduced from 2.46 to 2.23 (10%) while at the higher temperature of 102 °C the decrease is slightly less, going from 2.51 to 2.31 (9%). The source of this enhanced strain hardening is still not entirely clear but the work of Riggleman et al. [14] provides a possible explanation. In their study, observations of the effects of nanoparticles on the entanglement network of a

polymer nanocomposite using molecular simulations were reported. It was suggested that nanoparticles can serve as entanglement attractors, trapping and perturbing the primitive paths of the polymer chains more effectively as the deformation proceeds, leading to a significant enhancement of the entanglement network (good polymer-particle interaction was a necessary pre-requisite for this effect). This entanglement nucleator effect should mean that as the degree of exfoliation increases so also should the nucleator effect, which would be evident in the earlier onset of strain hardening. Figure 3 in section 3.3 shows TEM images for the unstretched and stretched PET-nanocomposites, while Table 4 contains the structural data from these images plus the calculated average aspect ratios. It is clear that the lower stretching temperature results in better delamination of tactoids and an increase in aspect ratio (increased viscosity occurring at lower temperatures leads to the development of higher tensile stresses). This is then reflected in a lower value of SHP supporting the entanglement nucleator effect.

The enhancement in strain hardening with the addition of clay means that higher forming forces will be required to deform the PET-clay materials. In an industrial context, if the forming stress is too high for the injection stretch blow moulding machine then a processor/operator will consider increasing the preform temperature. It can be seen in Figure 1 that increasing the temperature to 102 °C brings the forming stress of the nanocomposites down to a level similar to the unfilled PET. However, as seen from Table 4, the aspect ratio is lower for the sheet produced at the high temperature and as shown in section 3.5, this is accompanied by an expected reduction in mechanical performance. Therefore, increasing the forming temperature is not a recommended method to reduce forming stress when processing PET-clay nanocomposites unless an accompanying

reduction in properties is acceptable. A further reason to resist increasing temperature is that enhanced strain hardening behavior leads to products with more uniform wall thickness, which is beneficial in reducing the weight of products. For example, currently there is too much unnecessary material in the base of bottles for carbonated beverages. If the distribution of wall thickness can be improved, then less material will be needed. Figure 2 shows the effect of changing the strain rate on the biaxial deformation behaviour of PET and PET-clay nanocomposites stretched at a temperature of 102 °C, to a stretch ratio of 3. As one would expect, the stress increases as strain rate increases for the unfilled PET with the SHP reducing by 8% at the higher strain rate. On the other hand, the increase in strain rate has a lesser effect on the PET-clay nanocomposites. It is proposed that at the low strain rate there is more time for rotation of tactoids into the flow direction and subsequent delamination of clay tactoids under tensile stress which then act as entanglement nucleators increasing the strain hardening effect. This would result in a higher aspect ratio for the low strain rate sample, which is indeed the case as shown in Table 4, and a less than expected difference in the strain hardening behavior between the two strain rates. A further effect of increasing strain rate is the possibility of adiabatic heating which can lead to material softening at increasing strain rates [15]. The presence of clay particles is likely to increase frictional dissipation thus making it more likely to have adiabatic heating in the PET-clay materials. This effect has been observed in polyamide-clay systems [16]. If significant adiabatic heating is present in the PET-clay sample stretched at 2 s^{-1}, this would have the effect of reducing the difference of deformation behaviour between it and the material stretched at 1 s^{-1} when compared with the effect of strain rate on the unfilled PET material.

Further work at a greater range of strain rates and temperatures will need to be conducted to verify this hypothesis.

3.3 Morphological analysis

TEM images of biaxially stretched samples at a stretch ratio of 3, and at different temperatures and strain rates are shown in Figure 3. It is clear that the clay particles in all nanocomposites are well aligned and parallel to film surface after biaxial stretching regardless of the difference in temperature and strain rate. Table 4 shows the average tactoid thickness and length of compression moulded and biaxially stretched nanocomposites. The nanocomposites after biaxial stretching show significantly lower average tactoid thickness and length compared with the compression moulded samples. This indicates that biaxial stretching has effectively broken up the large tactoids into smaller and thinner tactoids. The samples stretched at 95°C have a higher aspect ratio which is likely due to the higher stresses transmitted to the clay at a lower temperature resulting in delamination of the tactoids and a consequent increase in aspect ratio.

It is evident from Figure 4 that there are similarities in the distributions of clay tactoid thickness for the films stretched at 102 °C with different strain rates, while the films stretched at lower temperature (95 °C) with the same strain rate (1 s^{-1}) show a better dispersion of clays. There are approximately 5 % tactoids with a thickness of 0-2 nm in the sample stretched at 102 °C which increases to 22 % in the sample stretched at 95 °C. This shows that lowering the temperature is effective in breaking up large tactoids into smaller ones, and even exfoliating some single platelets.

3.4 Crystallinity

Crystallinity (X_c, %) results for the biaxially stretched samples are shown in Table 3. All the PET-clay nanocomposites have a lower crystallinity than the unfilled PET. This reduction in crystallinity has been proposed to result from a confinement effect, produced by the clay, on the crystallization of polymer chains [17]. The reduction in PET-clay nanocomposites crystallinity values could be expected to result in a reduction in material modulus and thus any improvements in nanocomposite modulus are not due to increasing crystallinity nucleated by the clay. Since crystallinity also influences barrier properties the improvement in barrier to be expected from the presence of the clay will be lessened by this reduction in crystallinity. There is little influence of processing conditions on the crystallinity of either the filled or unfilled materials.

3.5 Mechanical properties

Table 5 shows the tensile properties of the biaxially stretched and compression moulded samples. The tensile properties of all materials are enhanced after biaxial stretching due to a combination of molecular alignment and strain-induced crystallization. The elongation at break of the biaxially stretched PET is lower than that of the compression moulded sample due to the fact that the polymer has less potential for further deformation after biaxial stretching. Overall, the addition of clay increases the tensile modulus and strength of the biaxially stretched nanocomposites, these properties increasing with decreasing stretching temperature and/or increasing strain rate. The highest enhancement both in modulus and strength (44% and 31% respectively) is obtained at a stretching temperature of 95 °C and a strain rate of 1 s^{-1}. Although there is about a 30 % decrease in elongation in the presence of clay, the stretched nanocomposites still exhibit good ductility. There is a 20 % modulus enhancement in the nanocomposites stretched at a temperature of 95 °C and a strain rate of

1 s^{-1}, compared with the nanocomposites stretched at a temperature of 102 °C and the same strain rate. Likewise, a 24 % enhancement in tensile strength occurs in the nanocomposites stretched at a lower temperature and the same strain rate of 1 s^{-1}. This is in agreement with the structural morphology discussed previously, which shows a similar level of clay dispersion at different strain rates but a significantly different level of clay dispersion at different temperatures as shown in Table 4 and Figure 4.It can be observed from Figure 5 that there are good correlations between the tensile properties and the strain hardening parameter (SHP). The tensile modulus and strength both increase with decreasing SHP. Since the stretched PET at different stretching conditions has similar levels of crystallinity, the enhancement in the modulus and strength of the PET should be attributed to the enhancement in polymer orientation. The PET-clay nanocomposites exhibit a similar trend but with a steeper slope compared with the data points for PET. The enhancement in PET-clay modulus is likely to be due to a combined contribution from the clay and enhanced molecular orientation due to confinement effects imposed by the clay.

It is useful to compare experimental values with conventional composite model predictions to assess the effectiveness of the reinforcement and determine the presence of any so called “nano effect” due to enhanced properties in the region in close proximity to clay [18]. Many previous studies have applied the Halpin-Tsai model to predict the modulus of polymer-clay nanocomposites [18]. The model equation is defined as:

$$\frac{E}{E_m} = \frac{1 + 2(l/t)\eta\phi_f}{1 - \eta\phi_f} \tag{1}$$

$$\eta = \frac{E_f / E_m - 1}{E_f / E_m + 2(l/t)} \tag{2}$$

where E and E_m are the modulus of the composite and matrix, respectively, Φ_f is the volume fraction of filler, and E_f is the modulus of the filler, (l/t) represents the filler aspect ratio. This model assumes that the filler and polymer matrix are elastic, isotropic, strongly bonded and their properties in the composite are considered to be identical to that in the pure state. The filler is treated as a rectangular platelet of uniform size and shape and fully aligned, and filler-filler interactions are not considered. Although clay can be assumed aligned upon biaxial stretching as shown in the TEM images, incomplete exfoliation, which is the case in our nanocomposites, affects the predicted relative modulus since the modulus of a tactoid is much less than that of a single platelet (178 GPa [18]). The tensile modulus of a tactoid in the direction longitudinal to its platelets can be assumed by using the rule of mixtures [18]:

$$E_{tactoid} = \Phi_{platelet}E_{platelet}+\Phi_{gallery}E_{gallery} \quad (3)$$

$$\phi_{gallery} = \frac{(n-1)(d_{001} - t_{platelet})}{d_{001}(n-1)+t_{platelet}} \quad (4)$$

where $\Phi_{platelet}$ is the volume fraction of clay platelets in the tactoid, $E_{platelet}$ is the modulus of a clay platelet, $\Phi_{gallery}$ is the volume fraction of gallery space, $E_{gallery}$ is the modulus of the material in the gallery, n is the number of platelets per tactoid, d_{001} is the d-spacing measured from XRD, $t_{platelet}$ is the thickness of a clay platelet.

As $E_{gallery}$ is expected to be much less than $E_{platelet}$, $E_{tactoid}$ is often expressed as:

$$E_{tactoid} = \Phi_{platelet}E_{platelet} = (1-\Phi_{gallery})\, E_{platelet} \quad (5)$$

Using this equation it can be calculated, for example, that the modulus of a tactoid containing two platelets drops to about 107 GPa compared with the modulus of a single clay platelet at 178 GPa. When the number of platelets is more than ~10 or the tactoid

thickness is more than ~20, the tactoid modulus drops to a relatively constant value at around 80 GPa.

Figure 6 shows the comparison between the experimental and predicted modulus enhancement calculated using the Halpin-Tsai model with the modified tactoid modulus values calculated according to Equation 9. It should be noted that the prediction for the modulus of the compression moulded sample takes into account the fact that the alignment is random, and equation 10, based on the Laminate model, [19] is applied:

$$E_{random} = 0.49E_{\shortparallel} + 0.51E_{\perp} \quad (6)$$

where $E_{\shortparallel}$ and $E_{\perp}$ are the composites moduli in the directions longitudinal and transverse to the major axis of the fillers.The model predictions are a very good match to the experimental data except at 102 °C and 2 s^{-1} (i.e at an aspect ratio of 23) where the predicted modulus is significantly higher than the experimental value. It is not clear why this difference between predicted and actual modulus should occur for the high strain rate sample but one possible answer lies in the earlier suggestion that adiabatic heating is taking place in this sample. This would have the effect of reducing the molecular orientation in the PET-clay sample thus reducing the experimental modulus relative to the predicted value.

3.6 Barrier properties

Figure 7 shows the oxygen gas permeability coefficient of the materials investigated. There is a 27 % decrease in the oxygen gas permeability coefficient in the stretched PET-clay films compared with the stretched PET film. One might expect that the higher aspect ratio of the PET-clay sample stretched at 95 °C (aspect ratio of 31) would lead to a lower permeability coefficient than that for the 102 °C sample (aspect ratio of 27), however, the

predicted permeabilities using the Nielsen model [20] for NC951BS and NC1021BS are 2.7 and 2.8 respectively, which is an insignificant difference.

4 Conclusions

The addition of 6% clay to PET has little effect on the crystallinity or the temperature operating window of the compression moulded "preform" but it has a significant effect on its strain hardening behavior as previously reported [18]. This enhanced strain hardening is accompanied by an increase in the exfoliation of clay tactoids in the matrix and a consequent improvement in both tensile modulus and strength. The strain hardening parameter (SHP), determined from the stress-strain curves, is inversely and linearly correlated with tensile modulus and strength for both the unfilled PET and PET-clay nanocomposites with the slope being greater for the PET-clay materials. SHP in both PET and PET-clay nanocomposites decreases with decreasing temperature or increasing strain rate. The decrease in SHP is accompanied by an increase in average particle aspect ratio, except for the sample stretched at the higher strain rate of 2 s^{-1}. It is proposed that higher strain rates inhibit the rotation of the clay tactoids along the stretching direction, thus reducing the potential for delamination during subsequent stretching. Decreasing the stretching temperature has a significant positive effect on particle aspect ratio, mechanical and O_2 barrier properties of the PET-clay material while increasing strain rate has a lesser effect. Molecular relaxation due to adiabatic heating is proposed as a potential reason for the different effects of strain rate on the unfilled and filled materials. This would explain the reduced modulus of the higher strain rate PET-clay sample which is lower than that predicted by the Halpin-Tsai model. Apart from the higher strain rate sample, the enhancement in tensile modulus of the PET-clay materials relative to the unfilled PET is

accurately predicted by the Halpin-Tsai model if a modified particle modulus (rather than the nominal clay modulus), based on average particle thickness, is used. In terms of the commercial benefits of the use of nanoclays in packaging materials it might be argued that the barrier and modulus enhancement values do not justify the extra cost of the clay addition, however, this view will change as the economic and legislative environmental climate change. It should be noted that a 44% increase in modulus will in theory allow a wall thickness reduction (and pack weight) of approximately 13%. This is a very significant material saving that would be accompanied by a proportional decrease in the energy required to process and transport the material. With today's quest for reduced environmental impact of packaging this provides an added incentive to consider the use of nanoparticles in polymer products.

Acknowledgements

The authors would like to thank (EPSRC) UK for funding this work.

References

[1] Paul DR, Robeson LM. Polymer nanotechnology: Nanocomposites. Polymer 2008; 49: 3187-3204.

[2] Chavarria F, Shah RK, Hunter DL, Paul DR. Effect of Melt Processing Conditions on the Morphology and Properties of Nylon 6 Nanocomposites. Polymer Engineering and Science 2007; 47: 1847-1864.

[3] Homminga D, Goderis B, Hoffman S, Reynaers H, Groeninckx G. Influence of shear flow on the preparation of polymer layered silicate nanocomposites. Polymer 2005; 46: 9941-9954.

[4] Giraldi ALF de M, Bizarria MTM, Silva AA, Mariano C, Velasco JI, d'Avila MA, Mei LHI. Effect of Clay Content and Speed Screw Rotation on the Crystallisation and Thermal Behaviours of Recycled PET/Clay Nanocomposites. Journal of Nanoscience and Nanotechnology 2009; 9: 3883-3890.

[5] Lertwimolnun W, Vergnes B. Influence of compatibilizer and processing conditions on the dispersion of nanoclay in a polypropylene matrix. Polymer 2005; 46: 3462-3471.

[6] Dintcheva NT, Marino R, Mantia FP. The role of the matrix-filler affinity on morphology and properties of polyethylene/clay and polyethylene/compatibilizer/clay nanocomposites drawn fibers. E-Polymers 2009; 054.

[7] Abu-Zurayk R, Harkin-Jones E, McNally T, Menary G, Martin PJ, Armstrong CG. Biaxial deformation behavior and mechanical properties of a polypropylene/clay nanocomposite. Composites Science and Technology 2009; 69: 1644-1652.

[8] Soon K, Harkin-Jones E, Rajeev RS, Menary G, McNally T, Martin PJ, Armstrong CG. Characterisation of melt-processed poly(ethylene terephthalate)/ syntheticmica nanocomposite sheet and its biaxial deformation behaviour. Polymer International 2009; 58: 1134-1141.

[9] Jeol S, Fenouillot F, Rousseau A, Marsenelli-Varlot K, Gauthier C, Briois JF. Drastic Modification of the Dispersion State of Submicron Silica during Biaxial Deformation of Poly(ethylene terephthalate). Macromolecules 2007; 40: 3229-3237.

[10] Martin PJ, Tan CW, Tshai KY, McCool R, Menary G, Armstrong CG. Biaxial characterization of materials for thermoforming and blow molding. Plastics, rubber and composites 2005; 34: 276-282.

[11] Fann D, Huang S, Lee J. Kinetics and thermal crystallinity of recycled PET. II. Topographic study on thermal crystallinity of the injection-molded recycled PET. Journal of Applied Polymer Science 1996; 61: 261-271.

[12] Bizarria MTM, Giraldi ALF de M, de Carvalho CM, Velasco JI, d'Avila MA, Mei LHI. Morphology and Thermomechanical Properties of Recycled PET-Organoclay Nanocomposites. Journal of Applied Polymer Science 2007; 104: 1839-1844.

[13] Chandran P, Jabarin S. Biaxial Orientation of Poly (ethylene Terephthalate). Part II: The Strain-Hardening Parameter. Advances in Polymer Technology 1993; 12: 133-151.

[14] Riggleman RA, Toepperwein G, Papakonstantopoulos GJ, Barrat JL, de Pablo JJ. Entanglement network in Nanoparticle Reinforced Polymers. The Journal of Chemical Physics 2009; 130: 244903.

[15] Zaroulis JS, Boyce MC. Temperature, strain rate, and strain state dependence of the evolution in mechanical behaviour and structure of poly(ethylene terephthalate) with finite strain deformation. Polymer 1997; 38: 1303-1315.

[16] McNally T, Murphy WR, Lew CY, Turner RJ, Brennan GP. Polyamide-12 layered silicate nanocomposites by melt blending. Polymer 2003; 44: 2761-2772.

[17] Harrats C, Groeninckx G. Features, Questions and Future Challenges in Layered Silicates Clay Nanocomposites with Semicrystalline Polymer Matrices. Macromolecular Rapid Communications 2008; 29: 14-26.

[18] Fornes TD, Paul DR. Modeling properties of nylon 6/clay nanocomposites using composite theories. Polymer 2003; 44: 4993-5013.

[19] Hull D, Clyne TW. An introduction to composite materials. 2nd Edition, Cambridge University Press 1996.

[20] Nielsen LE. Models for the permeability of filled polymer systems. Journal of Macromolecular Science 1967; 1: 929-942.

Figures captions

Figure 1: Biaxial deformation behaviour of PET and PET-clay nanocomposites stretched at a strain rate of 1 s^{-1}, to a stretch ratio of 3, and at different temperatures.

Figure 2: Biaxial deformation behaviour of PET and PET-clay nanocomposites stretched at 102 °C, to a stretch ratio of 3, and at different strain rates.

Figure 3: TEM images of (a) NCCM, (b) NC1021BS, (c) NC1022BS, (d) NC951BS.

Figure 4: Distribution of clay tactoid thickness.

Figure 5: (a) Tensile modulus and (b) strength as a function of strain hardening parameter.

Figure 6: Experimental and predicted relative modulus as a function of aspect ratio.

Figure 7: Oxygen gas permeability coefficients of PET and PET-clay nanocomposites.

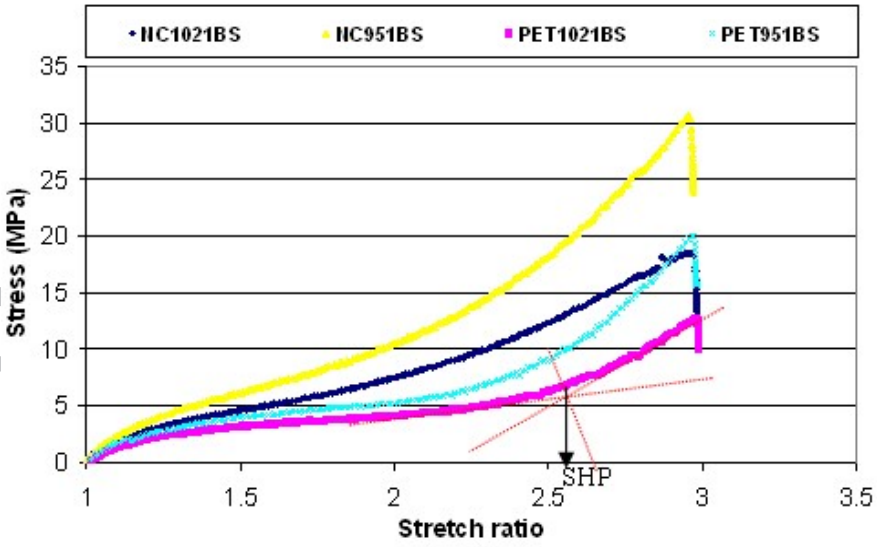

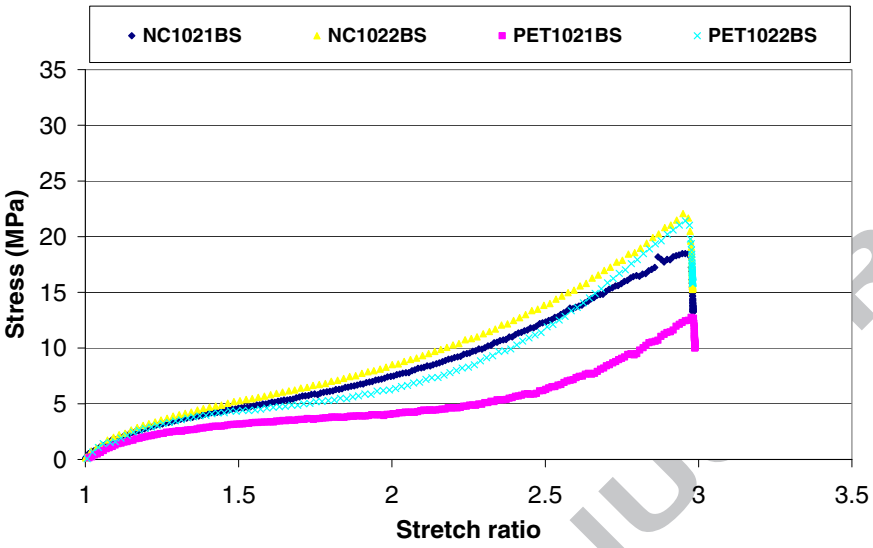
NC1021BS
NC1022BS
PET1021BS
PET1022BS
Stress (MPa)
Stretch ratio
0
5
10
15
20
25
30
35
1
1.5
2
2.5
3
3.5

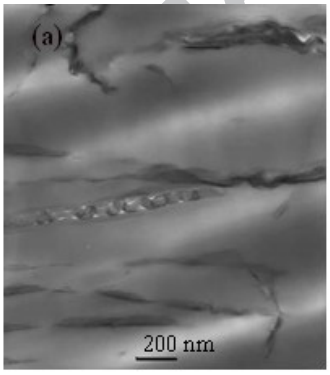
(a)
200 nm

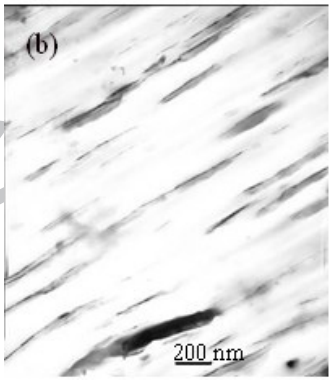
(b)
200 nm

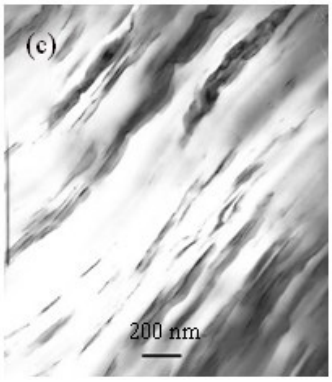
(c)
200 nm

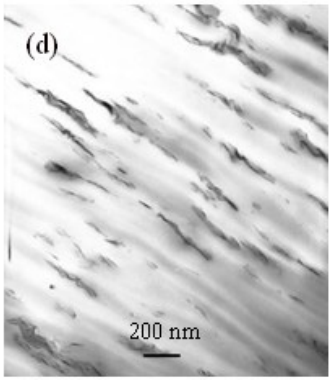
(d)
200 nm

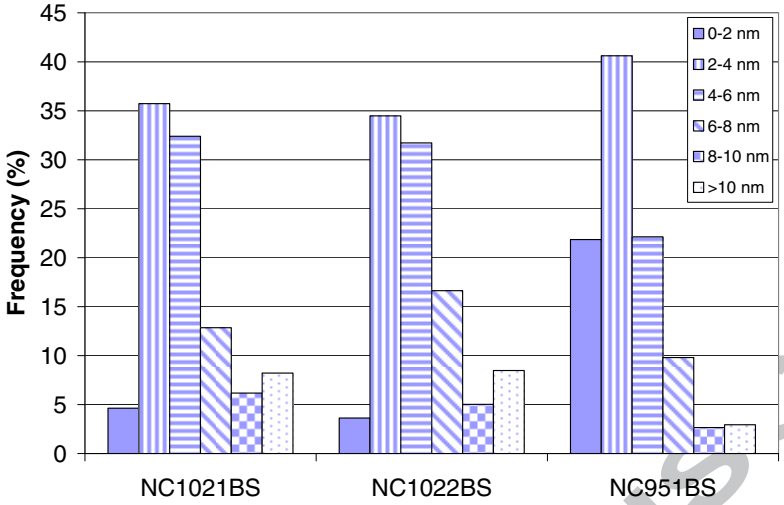

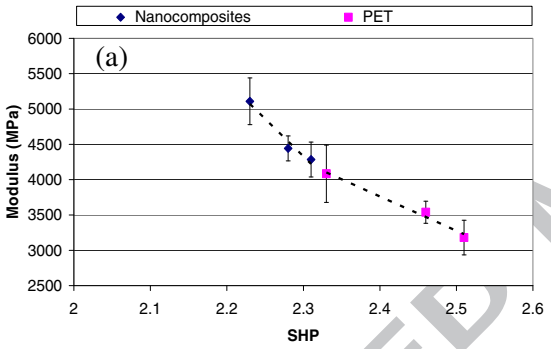

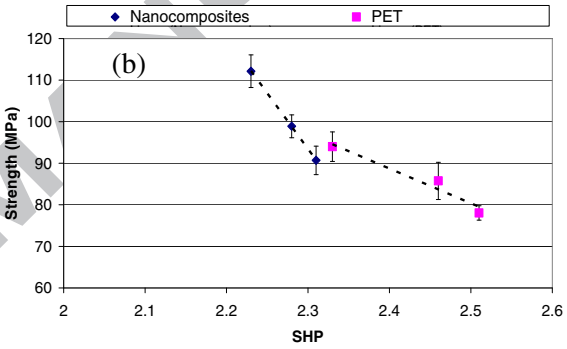

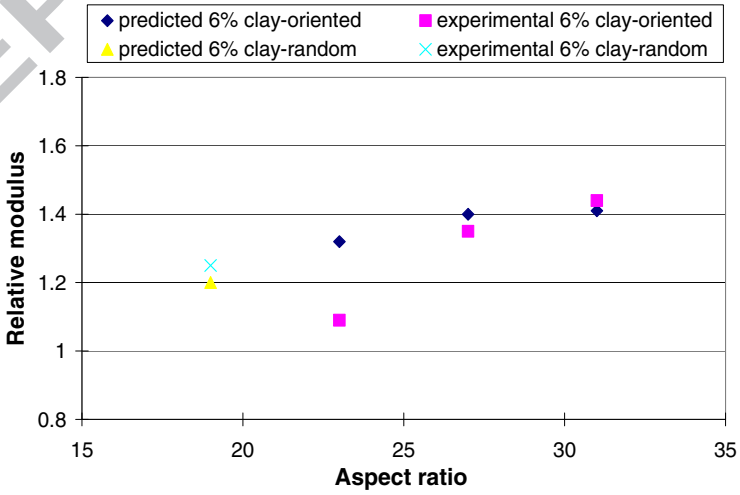

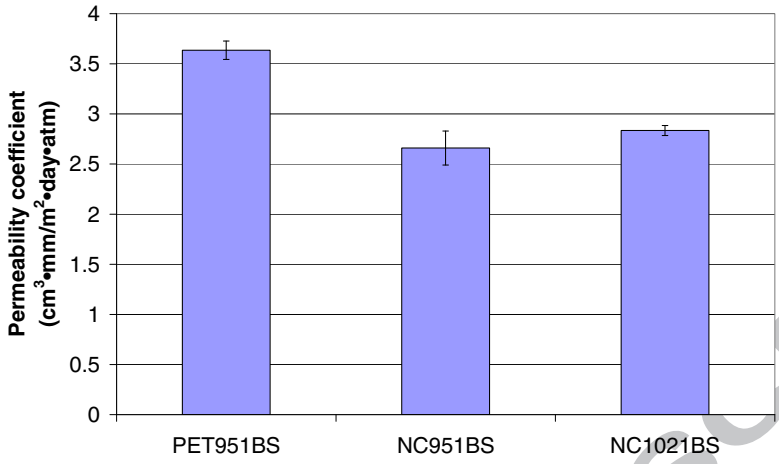

Table 1: Biaxial stretching parameters for PET samples (BS indicates biaxially stretched)

Sample	Sample code	Stretch Ratio	Strain Rate (s^{-1})	Temperature (°C)
N.C. (6%clay)	NC1021BS	3	1	102
	NC951BS	3	1	95
PET	NC1022BS	3	2	102
	PET1021BS	3	1	102
	PET951BS	3	1	95
	PET1022BS	3	2	102

Table 2: DSC and XRD results for compression moulded materials (CM indicates compression moulded)

Material	Sample code	X_c (%)	T_m (°C)	T_{cc} (°C)	T_g (°C)	d-spacing (Å)
SOMASIF	-	-	-	-	-	23.3
PET	PETCM	11 ±2	248.7 ±0.1	126.4 ±0.1	89.5 ±0.7	-
PET-clay	NCCM	12 ±2	248.9 ±0.8	124.1 ±0.3	88.5 ±0.6	22.7

Table 3: Values of strain hardening parameter and crystallinity for biaxially stretched samples

Sample code	NC1021BS	NC1022BS	NC951BS	PET1021BS	PET1022BS	PET951BS
SHP	2.31	2.28	2.23	2.51	2.33	2.46
Xc (%)	36	38	37	43	43	44

Table 4: Quantitative structural parameters for PET-clay nanocomposites

Sample code	Average Tactoid Thickness (nm)	Average Tactoid Length(nm)	Average Aspect Ratio
NCCM	20.1	383	19
NC951BS	4.2	132	31
NC1021BS	5.9	161	27
NC1022BS	6.0	138	23

Table 5: Tensile properties of biaxially stretched and compression moulded samples

Sample code	Modulus (MPa)	Effect on modulus of PET (%)	Strength (MPa)	Effect on strength of PET (%)	Elongation (%)	Effect on elongation of PET (%)
PET1021BS	3181 ±245	35 [a]	78.1 ±1.7	16	114.4 ±16.3	-34
NC1021BS	4285 ±246		90.7 ±3.4		76.0 ±34.0	
PET1022BS	4083 ±406	9	94.0 ±3.6	5	83.4 ±14.4	-23
NC1022BS	4442 ±177		98.9 ±2.8		64.6 ±10.4	
PET951BS	3539 ±157	44	85.8 ±4.5	31	109.4 ±13.1	-31
NC951BS	5109 ±330		112.2 ±3.9		75.8 ±12.8	
PETCM	2897 ±155	25	49.5 ±2.5	-24	613.1 ±173.4	-99
NCCM	3610 ±236		37.8 ±2.2		1.9 ±0.4	

([a] Effect on modulus of PET is calculated as: (4285-3181)*100% / 3181, likewise for others.

Positive value indicates enhancement, negative value indicates reduction)